Carrier localization and the origin of luminescence in cubic InGaN alloys

P. R. C. Kent and Alex Zunger

Citation: Applied Physics Letters **79**, 1977 (2001); doi: 10.1063/1.1405003
View online: http://dx.doi.org/10.1063/1.1405003
View Table of Contents: http://scitation.aip.org/content/aip/journal/apl/79/13?ver=pdfcov
Published by the AIP Publishing

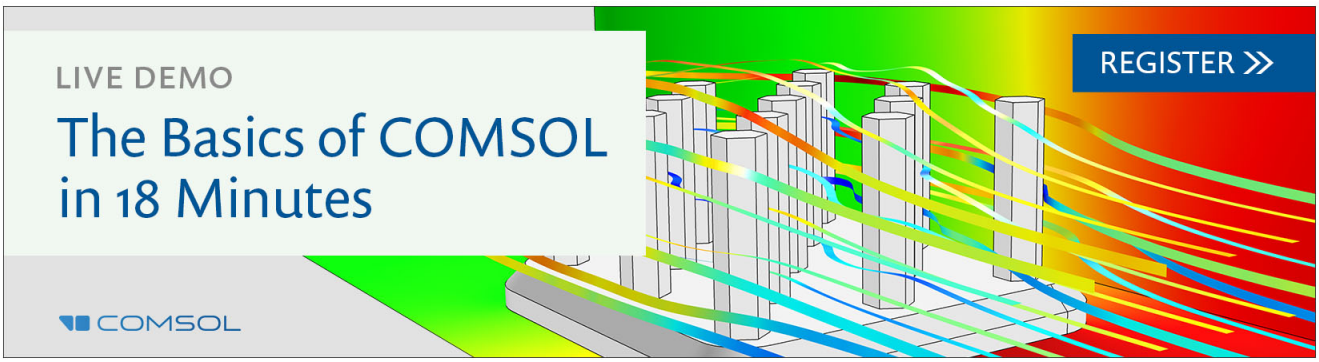

Carrier localization and the origin of luminescence in cubic InGaN alloys

P. R. C. Kent[a] and Alex Zunger
National Renewable Energy Laboratory, Golden, Colorado 80401

(Received 15 May 2001; accepted for publication 31 July 2001)

The electronic structure and optical properties of cubic (nonpiezoelectric) InGaN are investigated using large scale atomistic empirical pseudopotential calculations. We find that (i) strong hole localization exists even in the homogeneous random alloy, with a preferential localization along the [1,1,0] In–N–In–N–In chains, (ii) even modest sized (<50 Å) indium rich quantum dots provide substantial quantum confinement and readily reduce emission energies relative to the random alloy by 200–300 meV, depending on size and composition, consistent with current photoluminescence, microscopy, and Raman data. The dual effects of alloy hole localization and localization of electrons and hole at intrinsic quantum dots are responsible for the emission characteristics of current grown cubic InGaN alloys. © *2001 American Institute of Physics.* [DOI: 10.1063/1.1405003]

The development and commercialization of InGaN-based optoelectronic devices has occurred despite a limited understanding of the underlying electronic structure and light emission mechanisms of this alloy.[1] Although relatively efficient emission has been achieved for the entire visible range, optimization based on an understanding of the underlying electronic structure is expected to substantially improve device performance. Current InGaN alloys exhibit numerous anomalous phenomena that have been interpreted as indicative of an unconventional electronic structure. The following have been observed experimentally: (i) highly efficient photoluminescence (PL), despite a high dislocation density,[1] (ii) discrete states of varying energy inside the band gap in both quantum wells and epilayers,[2,3] (iii) a large Stokes' shift between emission and absorption energies, in both cubic and wurtzite InGaN samples,[2] (iv) an S-like dependence of emission energy on temperature,[4] (v) persistent photoconductivity,[5] (PPC). Collectively, these phenomena are indicative of localized excitons. While many of the observed localization phenomena can be attributed to the strong electric polarization existing in the *wurtzite* alloy, measurements on *cubic* alloys,[2,3] that lack polarization by symmetry, have found that the above phenomena persist. Thus, polarization alone is insufficient to explain the localization properties of InGaN. In general, there are two classes of localization in crystalline semiconductor alloys: (a) localization occurs even in a spatially homogeneous alloy due to the microscopic difference in potentials of the alloyed atoms,[6,7] and (b) localization due to spatial inhomogeneity (e.g., clustering, dot formation).[8,9] Recent electron micrography[10] revealed highly nonuniform In distributions, primarily consisting of sub-100 Å ''dotlike'' regions of apparently very high In composition surrounded by larger regions of lower In composition. These observations have led to speculation that carrier localization at these In-rich ''intrinsic quantum dots'' [mechanism (b) above] is responsible for the efficient emission of these devices.[8,9,11]

Here, we report large scale, fully atomistic electronic structure calculations on cubic InGaN alloys, and provide an explanation for the current experimental observations of localization in terms of (a) emission due to hole localization extant in the perfectly homogeneous random alloy, and (b) emission from quantum confined states in intrinsic quantum dots. In order to investigate the electronic properties of InGaN alloys, we adopt a twofold strategy: First, we simulate perfectly random InGaN alloys using supercells containing random distributions of In atoms. Second, we simulate the effects of spontaneous dot formation by embedding In-rich spheres of varying In composition and diameter inside a lower In-content InGaN alloy. This approach permits us to separate the electronic consequences of random alloy fluctuations in compositionally homogeneous alloys from those due to ''intrinsic quantum dot'' formation.

To model the InGaN alloys and dots we use the methodology detailed in Refs. 12 and 13: *Random alloys* are modeled by randomly distributing In atoms onto the cation sites of a periodic zincblende GaN supercell consisting of 4096 atoms, dimension $\sim 36\times 36\times 36$ Å. Such random distributions create naturally[12,13] not only single In impurity sites, but also In pairs, chains, and clusters. Strain-minimizing atomic displacements ensuing from the In–Ga atomic size mismatch are incorporated using the valence force field approach. We assume that the lattice constant of the supercell varies linearly with In composition. In order to model the *intrinsic quantum dots* we use larger, $\sim 140\,000$ atom or $\sim 120\times 120\times 120$ Å, supercells to contain the larger-scale In-rich regions. The electronic structure of the relaxed supercells is then obtained via the modern version of the empirical pseudopotential method[14] (EPM). Unlike traditional EPM, this potential reproduces not only experimentally correct band gaps, but also effective masses, and interfacial band offsets. In addition, we use explicitly strain dependent pseudopotentials in order to accurately reproduce the deformation potentials for both valence and conduction band states and thus explicitly include the effect of internal strains in the material due to the large bond length mismatch. Wave functions are obtained in a plane-wave basis (thus, affording multiband coupling).

Electronic localization along [1,1,0] In chains in InGaN random alloys: We calculated the near-gap conduction and

[a]Electronic mail: paul_kent@nrel.gov

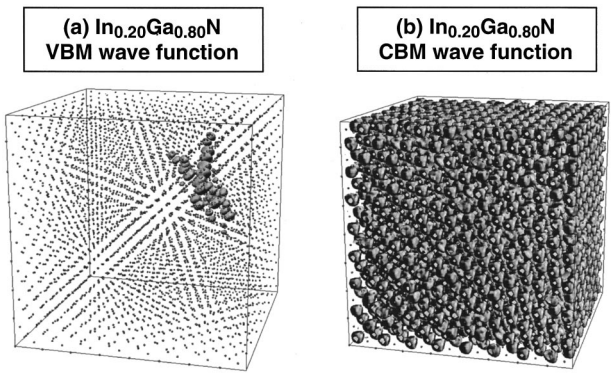

FIG. 1. Wave function squared of the uppermost valence and lowest conduction states of a 20% InGaN alloy, calculated using 4096 atom cells. The isosurfaces correspond to 75% of the integrated charge. The valence state is localized along the [1,1,0] crystallographic direction due to the statistical formation of [1,1,0] indium chains.

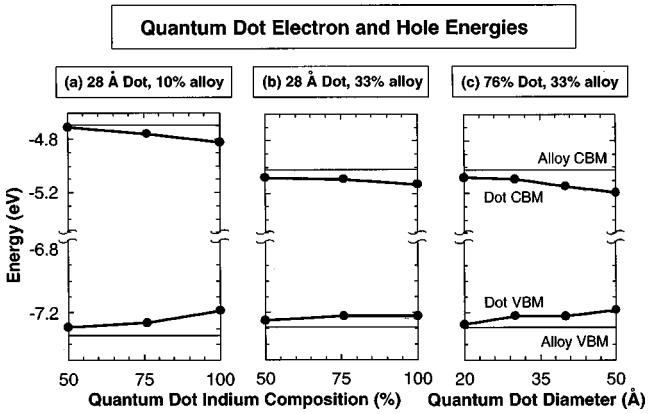

FIG. 2. Computed conduction and valence levels of In-rich quantum dots of varying size and composition embedded in a 33% InGaN random alloy. The lines drawn are a guide to the eye.

valence states of unstrained random alloys, averaging the results of 15 different randomly generated alloy configurations. Although no states are present within the gap at any concentration, we find a surprising localization of the valence states. Bellaiche *et al.*[12] demonstrated marked hole wave function localization, centered around In atoms, for very dilute InGaN alloys. In the present calculations using *higher* concentration alloys, we find hole localization extends across the entire device-relevant concentration range (at least up to 40%). Similar results were recently noted by Wang.[15]

Figure 1 compares the wave function isosurfaces of the highest valence state of a 10% InGaN alloy with the wave function of the lowest conduction state of the alloy. Atomic positions are shown as dots, whereas wave functions are shown as color isosurfaces. We observe strong hole localization of the valence state, whereas the conduction state is Bloch-like and delocalized across the entire supercell (this does not, however, imply inefficient electron-hole recombination). The InGaN localized valence states also exist for lower energies (up to 100–200 meV below the valence band maximum at 20%). Analysis of the *local In configurations* across the supercell, for different random alloy samples, revealed a preferential localization of holes on In-rich atomic chains oriented along the [1,1,0] crystallographic axes: While the overall In concentration of our cells is fixed, random statistics naturally results in the formation of numerous In-rich and In-poor regions, including randomly occurring chains of In–N–In–N–In-. This preferential localization and formation of ''chain states'' occurs because the small size of the N atoms permits the next nearest neighbor atoms along the zig–zag zinc-blende [1,1,0] chain to closely approach to $R_{\mathrm{In-In}}=3.3-3.4\,\text{Å}$, close to the metallic $R=3.2-3.3\,\text{Å}$ value, strongly coupling the valence states. In InGaP alloys, the P atoms are larger so $R_{\mathrm{In-In}}=3.9-4.0\,\text{Å}$ and the interband couplings are significantly smaller, so localization along In–P–In–P–In chains does not occur. Note that in general [1,1,0]-oriented impurity pairs in semiconductors lead to the deepest and most localized energy states of all other pair orientations. This reflects that fact that the [1,1,0] direction is the only zinc blende lattice direction whose atomic bonds appear continuously, leading to strong coupling of electronic states along such bond chains.[16]

We conclude that hole localization of valence states in InGaN alloys occurs even in the absence of large-scale In clustering or phase segregation and represent the fact that randomly occurring In chains act as deep acceptors. This is important, since *bulk* segregation predicted by Ho *et al.*[17] is not expected to occur in *epitaxial* films grown from vapor phase due to the mechanism of surface-enhanced solubility[18] and epitaxy-enhanced solubility[19] that dramatically reduce phase segregation in the film, at least for $x<20\%$.

Quantum confinement and reduction in emission energy due to intrinsic quantum dots: We calculated the near-gap conduction and valence states of spherical In-rich quantum dots embedded in nominally unstrained random alloys of lower In content. This simple model for the In inhomogeneities is sufficient to provide an estimate of the size and composition of In-rich regions necessary to explain the low energy PL of cubic InGaN samples[3], which is one of the main aims of this work.

Figure 2 shows the calculated electron and hole energies for several different sizes and composition of In-rich quantum dot, embedded in In-poor alloys. We see that its gap decreases as the In composition increases in the alloy matrix. At the same time, the gap of the dot decreases too, with increasing In composition inside the dot [Figs. 2(a) and 2(b)], and with increasing dot size [Fig. 2(c)]. Overall, the dot has a smaller gap than the alloy (the alloy conduction band minimum and valence band maximum are shown as horizontal lines). There are four effects that contribute to the overall gap reduction, e.g., approximately for a 100% In, 28 Å dot in a 33% InGaN alloy: (i) The increased In concentration in the dot *lowers* its gap, by 474 meV, (ii) the compressive strain exerted by the alloy medium on the dot *increases* its gap, by 165 meV (calculated from the band gap of bulk InN strained by the average strain within the dot after relaxation). (iii) The quantum confinement of levels inside the dot *increases* its gap, by 71 meV. The sum of (i)–(iii) is given by the difference shown in Fig. 2 between the alloy medium band edges (horizontal lines) and those of the dot, 238 meV. (iv) Electron-hole attraction within the dot *reduces* its (excitonic) gap by 49 meV. This is calculated directly from the pseudopotential wave functions, screening the Coulomb potential as per Ref. 20. The sum of (i)–(iv) gives the net reduction in the dot gap with respect to the alloy medium,

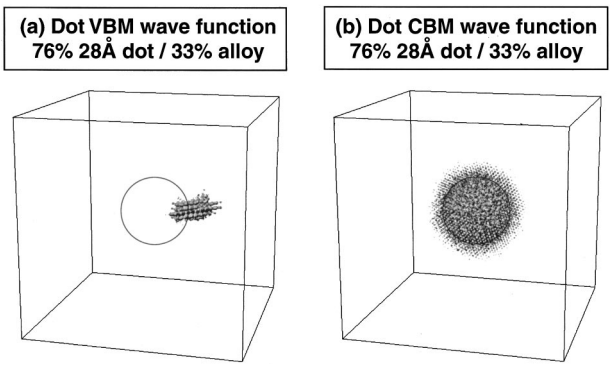

FIG. 3. Wave function squared of (a) the uppermost valence and (b) the first conduction state of a 76% InGaN spherical quantum dot of 28 Å diameter embedded in a 33% InGaN random alloy, calculated for 140 000 atom cells. The approximate edge of the dot is marked by a solid line. The isosurfaces correspond to 75% of the integrated charge.

287 meV. Thus, we find that the observed 240 meV reduction in gap in nominally 33% alloys[3] is consistent with ~ 28 Å dots of 100% In composition, and is also consistent with larger dots of lower composition, e.g., a 76% 40 Å dots. These estimates are in very good agreement with the Raman[3] and TEM[10] data, which estimate InN compositions of 76% and sizes $\leqslant 50$ Å, respectively, for different samples. For lower InN-content alloys we again find that small regions ($\leqslant 100$ Å) of high InN composition ($\geqslant 76\%$) reproduce the observed emission energies, although the dots must be somewhat larger or of higher In composition, e.g., for nominally 10% sample and 28 Å dots, an InN composition of 100% reduces the single particle gap by 292 meV, while a larger, 50 Å dot reduces the single particle gap by 742 meV.

Figure 3 shows electron and hole wave functions for a 76% dot in a 33% alloy. We observe (i) Holes localized *around* the dot for all dot compositions. Holes preferentially localize on the [1,1,0] corners of the dots, with the exact location being strongly modified by strain and the random fluctuations in the In composition around the dot. (ii) Electrons are localized inside the dot due to quantum confinement, for dots larger than ~ 20 Å (or ~ 200 atoms) for pure InN dots. (iii) We calculate a nonzero transition dipole between hole and electron levels. This is because although the hole states are localized adjacent to the dots, there remains some spatial overlap.

Physical consequences of hole localization and quantum confinement: The following physical picture emerges for the different localization mechanisms at play in cubic InGaN alloys. (i) Efficient PL occurs despite dislocations due to quantum confined states at ''quantum dots'' and localized chain states outside dislocations. Comparatively small, e.g., 50 Å, dots reduce the effective band gap relative to the alloy medium by up to ~ 300 meV [Fig. 2(c)]. (ii) The states associated with these quantum dots may be observed in PL in certain geometries, e.g., thick epilayers, depending on growth conditions. (iii) A Stokes' shift between emission and absorption energies exists because, while emission occurs from the quantum dots, absorption occurs into the random alloy, which has a far greater density of states at higher energy. The observation of increasing Stokes' shift with nominal In content[21] is consistent with larger In-rich regions forming (thus emitting at lower energies) while the host alloy In composition remains comparatively pinned. (iv) An S-like dependence of PL energy with temperature,[4] due to thermalization of localized electrons and holes of varying localization and activation energy (depending on local In composition). Their activation, then depletion, with increasing temperature briefly dominates the overall downward trend of the alloy band gap. (v) PPC naturally occurs due to the existence of trapped holes in regions of moderate In composition: Increased temperatures activate these carriers, allowing them to tunnel to and recombine with electrons. The large variation in In composition, and consequently relatively deep traps, allows PPC to exist up to room temperature.[4]

We expect similar mechanisms of carrier localization to also exist in the wurtzite phase, due to the structural similarity between zincblende and wurtzite. Our cubic results must be modified for wurtzite, by the additional inbuilt and geometry dependent electric fields, which acts to separate carriers.

The demonstrated sensitivity of InGaN emission characteristics to the subtleties of very local indium arrangements (either random or due to growth) suggests that engineering of size controlled nanostructures, such as *intentionally grown* quantum dots, may provide a better route for optimization of emission characteristics than further optimization of alloy growth.

The authors thank S. F. Chichibu, L. W. Wang, and J. R. Leite for helpful discussions. This work is supported by the U.S. Department of Energy, SC-BES-OER Grant No. DE-AC36-98-GO10337.

[1] S. Nakamura and G. Fasol, *The Blue Laser Diode* (Springer, Berlin, 1997).
[2] S. F. Chichibu, T. Azuhata, T. Sota, and S. Nakamura, Appl. Phys. Lett. **76**, 1671 (2000).
[3] V. Lemos, E. Silveira, J. R. Leite, A. Tabata, R. Trentin, L. M. R. Scolfaro, T. Frey, D. J. As, D. Schikora, and K. Lischka, Phys. Rev. Lett. **84**, 3666 (2000).
[4] T. Y. Lin, J. C. Fan, and Y. F. Chen, Semicond. Sci. Technol. **14**, 406 (1999).
[5] H. C. Yang, T. Y. Lin, and Y. F. Chen, Appl. Phys. Lett. **78**, 338 (2001).
[6] S. Permogorov and A. Reznitsky, J. Lumin. **52**, 201 (1992).
[7] L. Bellaiche, Appl. Phys. Lett. **75**, 2578 (1999).
[8] S. Chichibu, T. Azuhata, T. Sota, and S. Nakamura, Appl. Phys. Lett. **69**, 4188 (1996).
[9] K. O'Donnell, R. Martin, and P. Middleton, Phys. Rev. Lett. **82**, 237 (1999).
[10] Y.-S. Lin, K.-J. Ma, C. Hsu, S.-W. Feng, Y.-C. Cheng, C.-C. Liao, C. C. Yang, C.-C. Chou, C.-M. Lee, and J.-I. Chyi, Appl. Phys. Lett. **77**, 2988 (2000).
[11] A. Wakahara, T. Tokuda, X.-Z. Dang, S. Noda, and A. Sasaki, Appl. Phys. Lett. **71**, 906 (1997).
[12] L. Bellaiche, T. Mattila, L.-W. Wang, S.-H. Wei, and A. Zunger, Appl. Phys. Lett. **74**, 1842 (1999).
[13] P. R. C. Kent and A. Zunger, Phys. Rev. Lett. **86**, 2613 (2001).
[14] A. Zunger, in *Quantum Theory of Real Materials*, No. 348 in *Kluwer International Series in Engineering and Computer Science*, edited by J. R. Chelikowsky and S. G. Louie (Kluwer Academic, Boston, 1996), p. 173.
[15] L. W. Wang, Phys. Rev. B **63**, 245107 (2001).
[16] K. Rustagi and W. Weber, Solid State Commun. **18**, 673 (1976).
[17] I.-H. Ho and G. B. Stringfellow, Appl. Phys. Lett. **69**, 2701 (1996).
[18] S. B. Zhang and A. Zunger, Appl. Phys. Lett. **71**, 677 (1997).
[19] D. M. Wood and A. Zunger, Phys. Rev. Lett. **61**, 1501 (1988).
[20] A. J. Williamson and A. Zunger, Phys. Rev. B **61**, 1978 (2000).
[21] R. W. Martin, P. G. Middleton, K. P. O'Donnell, and W. Van der Stricht, Appl. Phys. Lett. **74**, 263 (1999).